Available online at www.sciencedirect.com
ScienceDirect
Journal of Catalysis 243 (2006) 263–269
JOURNAL OF CATALYSIS
www.elsevier.com/locate/jcat

Steam reforming of acetic acid as a biomass derived oxygenate: Bifunctional pathway for hydrogen formation over Pt/ZrO_2 catalysts

Kazuhiro Takanabe [a], Ken-ichi Aika [b], Koji Inazu [a], Toshihide Baba [a], K. Seshan [c,*], Leon Lefferts [c]

[a] *Department of Environmental Chemistry and Engineering, Interdisciplinary Graduate School of Science and Engineering, Tokyo Institute of Technology, G1-14, 4259 Nagatsuta, Midori-ku Yokohama 226-8502, Japan*
[b] *Foundation for the Promotion of Science and Engineering, S2-10, 4259 Nagatsuta, Midori-ku, Yokohama 226-8503, Japan*
[c] *Catalytic Processes and Materials, Faculty of Science and Technology, Institute of Mechanics, Processes and Control Twente (IMPACT), University of Twente, P.O. Box 217, 7500AE, Enschede, The Netherlands*

Received 17 March 2006; revised 15 July 2006; accepted 18 July 2006

Available online 8 September 2006

Abstract

Mechanistic studies on steam reforming of acetic acid over Pt/ZrO_2 catalysts were performed as extension of our previous work [K. Takanabe, K. Aika, K. Seshan, L. Lefferts, J. Catal. 227 (2004) 101]. An overall picture of the bifunctional mechanism is established for steam reforming of acetic acid, where both Pt and ZrO_2 participate in the reaction. On Pt, bond breaking of acetic acid proceeds to form H_2, CO, CH_4, and CO_2 into gas phase, and to form the carbonaceous residue (most probably CH_x species), which can block Pt surface. Both pulse experiments as well as in situ IR data demonstrate that H_2O can be activated on ZrO_2 to create supplementary surface hydroxyl groups, which react to gasify the residue on Pt to give chiefly steam-reforming/water–gas shift products (H_2, CO_2), and thus the catalytic cycles continue. Importance of the Pt–ZrO_2 boundary sites is confirmed by the fact that the removal of the carbonaceous residue situated at the boundary sites results in catalyst regeneration.

Keywords: Steam reforming; Acetic acid; Acetone; Pt; ZrO_2; Mechanism; Bio-oil; Hydrogen; Sustainable

1. Introduction

The demand for hydrogen is expected to appreciate considerably in the coming years due to the rapid developments in fuel cell technology applications. There is tremendous interest in using hydrogen originating from renewable resources (e.g., biomass) to arrive at a CO_2-neutral energy supply [1]. Recent developments in flash pyrolysis has demonstrated that solid biomass made of lignocellulosic polymers can be efficiently converted to a liquid mixture, the so-called "bio-oil" [2], which allows easy transport followed by generation of hydrogen when needed. A combination of catalytic steam-reforming and water–gas shift (WGS) reactions can maximize hydrogen yield from bio-oil. Attempts to produce H_2 from bio-oil using commercial steam-reforming catalysts have been severely hindered by rapid catalyst deactivation caused by coke/oligomer deposition on the catalysts [3]. The mechanism of steam reforming of oxygenates has not been sufficiently elucidated to date [4,5], which has hampered the development of efficient and stable catalysts.

Bio-oil is a complex mixture of various aliphatic/aromatic oxygenates [6]. Thus, establishing the requirements for a catalyst is not straightforward. However, a more realistic approach would be to establish structure–activity correlations based on studies using individual components present in bio-oil. In this context, we have investigated steam reforming of acetic acid (CH_3COOH, AcOH) [7–9], one of the major components in bio-oil [10].

In earlier studies [7,8], we proposed that a bifunctional mechanism is involved in steam reforming of AcOH over supported Pt catalysts, where both Pt and the support participate in the catalysis. It has been shown that Pt is essential for hydrogen formation and that the support is needed to extend catalyst

* Corresponding author. Fax: +31 53 4894683.
E-mail address: k.seshan@utwente.nl (K. Seshan).

0021-9517/$ – see front matter
doi:10.1016/j.jcat.2006.07.020

life [7]. Further, in situ infrared spectroscopy measurements [7] support the hypothesis that boundary sites involving both Pt and the support are relevant to catalysis. Accordingly, we have shown that the concentration of such sites correlates linearly with the steam-reforming activity [8]. This is further supported by the fact that the Pt catalysts supported on different oxides give different intrinsic activities [8]. The differences have been tentatively suggested to be due to the varying water-activating ability of the oxides.

Mechanistic aspects of the steam reforming of hydrocarbons (especially methane) have been discussed extensively by other researchers. For instance, a bifunctional mechanism was proposed for steam reforming of methane and higher hydrocarbons by Rostrup-Nielsen for Ni-based catalysts [11,12]. In their proposal, hydrocarbons are adsorbed and activated primarily on the nickel sites, whereas water is adsorbed and activated on the support [11,12]. A similar bifunctional mechanism was also proposed for the dealkylation of toluene with steam, to benzene and syngas, over supported noble metal catalysts [13–16]. According to these studies, dissociative chemisorption of hydrocarbon occurs on Pt and surface hydroxyls derived from H_2O on the oxide support help to remove the hydrocarbon residue. Infrared spectroscopy has shown that surface hydroxyl groups on the support are consumed by reacting with toluene to produce oxygenated compounds (CO and CO_2) [17]. It is important to note that the role of the support in activating water has been stressed, especially when the metals Pt, Rh, and Pd were used [14–16]. The concept of the bifunctional mechanism has also been suggested for the WGS reaction, where CO adsorbs on the metal and water on the support [18].

In the case of steam reforming of oxygenates, however, the role of the support and the importance of boundary sites have not been clarified sufficiently. Thus, the aim of the present study was to clarify our proposed bifunctional mechanism during steam reforming of AcOH [7,8] with additional experimental results. An overall schematic pathway for steam reforming of AcOH based on sorption and reaction studies of AcOH and H_2O on the Pt/ZrO_2 catalysts is discussed. The role of the support is elucidated by focusing on the active species derived from H_2O and its reactivity.

2. Experimental

2.1. Catalyst preparation

ZrO_2 (monoclinic, Daiichi Kigenso Kagaku Kogyo, RC100) was first calcined for 15 h at 1125 K. It was then crushed and sieved to give grains of 0.3–0.6 mm diameter. An aqueous solution of $H_2PtCl_6{\cdot}6H_2O$ (Alfa Aesar, 0.01 g Pt per ml) and the calcined ZrO_2 grains were used to prepare catalysts with 0.5 wt% Pt loading. The Pt/ZrO_2 catalyst was dried and finally calcined for 15 h at 925 K. The specific surface areas were 21 $m^2\,g^{-1}$ for the ZrO_2 catalyst and 20 $m^2\,g^{-1}$ for the Pt/ZrO_2 catalyst. A Pt dispersion of 0.84 (H/Pt) was determined by hydrogen chemisorption. Pt black (Nilaco Co, 99.98%, 300 mesh) was used as a catalyst with no support, without further purification.

2.2. Catalytic measurements

For continuous tests, a 10- or 50-mg catalyst sample was loaded in a fixed-bed reactor and held by quartz wool plugs. The catalyst was first reduced in 5% H_2 in N_2 with a total flow rate of 50 ml min^{-1} at 775 K for 1 h. Then the reactor was purged with N_2 at a flow rate of 50 ml min^{-1}. An aqueous solution of AcOH or acetone giving a steam-to-carbon molar ratio (S/C) of 5 was introduced using a microfeeder and a syringe. AcOH and acetone were fed, giving a vapor pressure of 2.5 and 1.7 kPa, respectively. Total gas hourly space velocity (GHSV) of 320,000 or 1,600,000 h^{-1} was achieved with argon as a carrier gas. N_2 was added as an internal standard. The system was heated at 423 K to avoid condensation of reactants and products. After purging with inert gas (Ar), the mixture of reactants was introduced to the reactor. After the reaction, the catalysts were purged with Ar at the reaction temperature, cooled, and used for subsequent characterization. Analyses were done by gas chromatography (GC) using a Shimadzu model GC-14B equipped with both a Porapak Q column connected to a flame ionization detector for AcOH, acetone (CH_3COCH_3), and hydrocarbons as well as an active carbon column connected to a thermal conductivity detector for H_2, N_2, CO, CH_4, and CO_2.

The overall reaction stoichiometry for the conversion of AcOH to hydrogen can be drawn as Eq. (1), a combination of steam reforming and WGS [Eq. (2)]:

$$CH_3COOH + 2H_2O \rightarrow 2CO_2 + 4H_2, \tag{1}$$

$$CO + H_2O \rightleftarrows CO_2 + H_2. \tag{2}$$

In the case of acetone (product of AcOH ketonization) reforming, the reaction stoichiometry is

$$CH_3COCH_3 + 5H_2O \rightarrow 3CO_2 + 8H_2. \tag{3}$$

The hydrogen yields were calculated based on Eqs. (1) or (3). For carbon-containing compounds, the yields were calculated based on C_1 equivalent values; for example, acetone (C_3H_6O) yield was calculated as three times the number of moles produced divided by two times the number moles of AcOH fed [7].

Pulse experiments were performed with 20 mg of Pt/ZrO_2 or ZrO_2. After reduction at 775 K, the system was purged with Ar at a flow rate of 37.5 ml min^{-1}. After cooling down the catalysts to the reaction temperature (625 K), the required pulses of AcOH (3.8 μmol), H_2O (22 μmol), or O_2 (8.9 μmol) were injected. These analyses were done using a Shimadzu GC-8A gas chromatograph with the same types of columns and detectors as for the continuous test. The column was mounted in-line to the pulse reactor, so that all of the components in the exit gas mixture were separated and then analyzed quantitatively. The errors in these experiments were ±0.05 μmol.

To understand the kinetic relevance of secondary reactions that can occur during the conversion of AcOH, the Pt/ZrO_2 catalysts were tested for steam reforming of methane (CH_4/H_2O) and CO hydrogenation (CO/H_2). For these reactions, carbon partial pressure was kept at 5.1 kPa, and the gas mixture was fed at ratios of 5 for H_2O/C and 3 for H_2/C. The GHSV of 1,600,000 h^{-1} was achieved by dilution with Ar. Products were analyzed as described above.

2.3. Catalyst characterization

IR spectra were recorded in situ under vacuum by using JASCO FTIR620 spectrometer equipped with an MCT detector in transmission mode. A 100-mg catalyst pellet was loaded into a miniature cell equipped with CaF_2 transparent windows. The cell can be evacuated to pressures below 10^{-4} Pa. The catalyst was first reduced in situ by introducing 1 kPa of H_2 at 775 K. Then it was cooled down to 625 K, and the necessary spectra were recorded. Each spectrum, comprising 128 scans taken at 4 cm^{-1} resolution, was collected 5 min after the required gas was introduced or evacuated.

Temperature-programmed oxidation (TPO) measurements were carried out with catalyst samples (20 mg of ZrO_2 and Pt/ZrO_2 and 100 mg of Pt black) after exposure to AcOH pulses (3.8 μmol) and also after 1 h of continuous operation, to investigate the nature of the carbonaceous deposits. After the reactions, the catalysts were rapidly cooled from 625 to 373 K (typically within 120 s). Then the gas was switched to 5% O_2/He, and the catalysts were heated up to ca. 800 K. Carbonaceous deposits were oxidized to CO_x, which passed through a methanator and was finally detected with a flame ionization detector.

3. Results and discussion

3.1. Continuous catalytic tests

Table 1 shows results for steam reforming of AcOH over Pt/ZrO_2 catalyst. As reported in our previous work for the reaction at higher temperatures [7,9], the catalyst showed good activity for steam reforming even at 625 K at initial times on course. The products observed were H_2, CO_2, and CO, along with CH_4 and acetone. Separate experiments on ZrO_2 have already demonstrated [7,9] that acetone is formed via ketonization of AcOH over ZrO_2,

$$2CH_3COOH \rightarrow CH_3COCH_3 + CO_2 + H_2O. \quad (4)$$

The carbon mass balance was at least 25% deficient, suggesting that carbonaceous deposits remained on the catalyst. Steam reforming of acetone over Pt/ZrO_2 was also studied under comparable conditions (Table 1) because acetone is formed as a product from AcOH over ZrO_2. The data given in Table 1 show that acetone indeed can be steam reformed, although the level of conversion is about an order of magnitude lower; however, greater carbon loss (<30%) was observed. Our earlier work [7,9] suggested that this was due to aldol condensation-type reactions of acetone on the support to form deposits. In the present study, after 25 min time on stream, formation of hydrogen (as an indication of steam-reforming activity) was strongly suppressed (not shown). Because treatment in O_2 of the catalyst regenerates activity, we suggest that the loss of activity is due to blockage of the active sites for steam reforming by carbonaceous deposits.

Table 1
Steam reforming of AcOH and acetone over Pt/ZrO_2 catalyst at 5 min time on stream (625 K, $H_2O/C = 5$, GHSV = 320,000 h^{-1}, AcOH = 2.5 kPa or acetone = 1.7 kPa)

Reactant	Conversion (%)	Yield (%)					
		H_2	CO_2	CO	CH_4	Acetone	C_1 loss
AcOH	46.2	8.2	7.6	8.7	3.3	6.5	22
Acetone	27.0	1.2	0.8	0.1	<0.1	–	26

3.2. Catalytic cycle during steam reforming of acetic acid

A series of pulse reactions with AcOH and/or H_2O were carried out over the Pt/ZrO_2 catalysts. Note that the amount of AcOH in a single pulse corresponds to the amount introduced in the continuous test (Section 3.1) for less than 2 s.

Table 2 compiles results from pulse experiments with AcOH/H_2O and AcOH only over fresh Pt/ZrO_2 and ZrO_2 at 625 K. The results were similar to those reported for the reaction at 725 K [7] and are briefly described as follows. Over Pt/ZrO_2, the products observed from AcOH in the presence or absence of H_2O were H_2, CO_2, CO, CH_4, and acetone. Further, the presence of water caused a WGS reaction [Eq. (2)]. Ketonization of AcOH to form acetone and CO_2 [Eq. (4)] took place over ZrO_2, and no H_2 was formed, confirming that the presence of Pt is essential for the formation of H_2 [7]. Less acetone than CO_2 was observed [as would be expected from the reaction stoichiometry in Eq. (4)], due to consecutive conversion of acetone to oligomers. In all cases, significant carbon loss was observed (nearly 50% on a molar carbon basis).

The deposits deactivated the Pt surface, as demonstrated by the fact that hydrogen formation over Pt/ZrO_2 was strongly suppressed during subsequent AcOH pulses (indicated as "without

Table 2
Product distributions from AcOH pulse reaction, and conversion of deposits derived from AcOH with H_2O and O_2 (625 K, AcOH 3.8 μmol, H_2O 22 μmol, O_2 8.9 μmol)

Catalyst	Reactant	Yield (μmol)					Carbon deposit[a] (μmol)	Total C in products (μmol)
		H_2	CO_2	CO	CH_4	Acetone		
Pt/ZrO_2	AcOH/H_2O	1.85	2.01	0.08	1.26	0.14	3.7	–
Pt/ZrO_2	AcOH	1.32	0.91	1.57	0.75	0.26	3.0	–
ZrO_2	AcOH	0	0.74	0	0	0.35	3.7	–
Pt/ZrO_2	(AcOH →) H_2O[b]	0.73	0.40	0.04	0.05	0	2.5[c]	0.5
Pt/ZrO_2	(AcOH →) O_2[b]	0.06	3.04	0.06	0.01	0	0[c]	3.1

[a] Estimated from carbon balance.
[b] H_2O or O_2 was injected after 15 s from AcOH pulse.
[c] Carbon remaining on the catalysts.

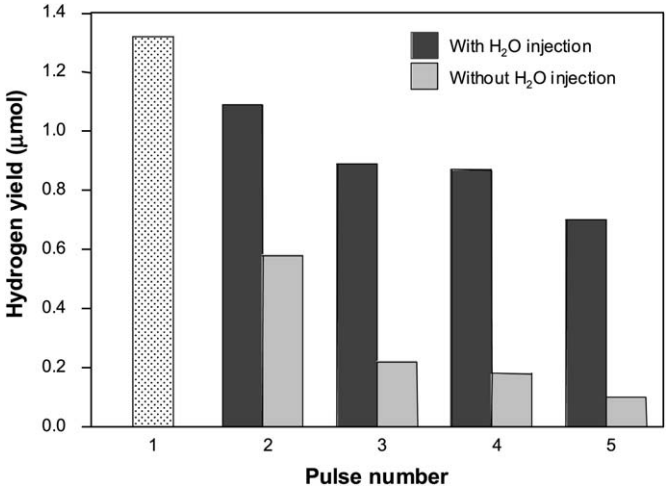

Fig. 1. Effects of H_2O injection after AcOH pulse on hydrogen yield over Pt/ZrO_2. H_2O pulse was injected 15 s after the AcOH pulse. (625 K, AcOH pulse 3.8 μmol, H_2O pulse 22 μmol.)

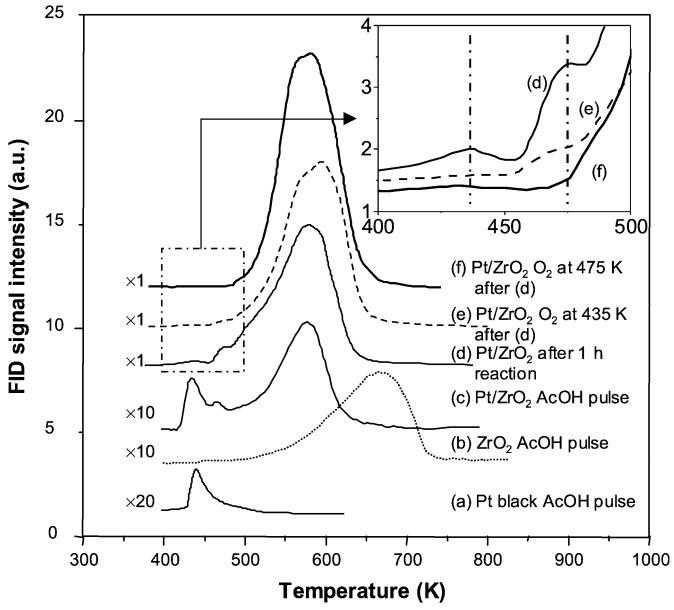

Fig. 2. Temperature programmed oxidation profiles of the catalysts used for the different reactions. (a) Pt black exposed to AcOH pulse, (b) ZrO_2 exposed to AcOH pulse, (c) Pt/ZrO_2 exposed to AcOH pulse, (d) Pt/ZrO_2 after 1 h reforming, (e) sample d treated in O_2 at 435 K after 15 min, (f) sample d treated in O_2 at 475 K. (AcOH pulse 3.8 μmol, Reforming conditions: 625 K, $H_2O/C = 5$, GHSV = 320,000 h^{-1}, AcOH = 2.5 kPa.)

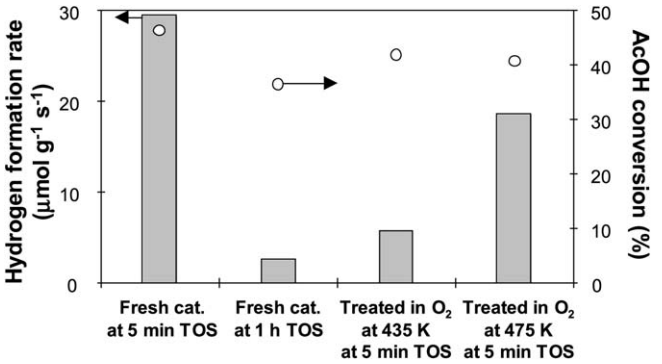

Fig. 3. Effects of O_2 treatment on hydrogen formation rate over Pt/ZrO_2 after deactivation. (625 K, $H_2O/C = 5$, GHSV = 320,000 h^{-1}, AcOH = 2.5 kPa.)

H_2O injection" in Fig. 1). Thus, water as a coreactant should play an important role in cleaning up deposits on the Pt surface for the subsequent decomposition of AcOH (at least partially). When a water pulse was introduced immediately (15 s) after each AcOH pulse injection, a part of the remaining species on the catalyst derived from an AcOH pulse (0.5 out of a 3.0 μmol C base) was gasified to form chiefly H_2 and CO_2 as a consequence of steam reforming and WGS (Table 2). Indeed, Fig. 1 shows ("with H_2O injection") that the water treatment greatly improved the durability for hydrogen formation. This can be an indication of the catalytic cycle during steam reforming of AcOH; AcOH decomposes on Pt to give H_2, CO_x, and CH_4 and some carbonaceous deposits covering the Pt surface, and subsequently the deposits are gasified with H_2O to form H_2 and CO_x and also to make the Pt surface available for the next AcOH turnover (i.e., decomposition).

3.3. Selective removal of deposits and its relevance to steam-reforming activity

All of the deposits formed after pulse reaction with AcOH on the Pt/ZrO_2 were gasified to CO_2 with oxygen at 625 K (Table 2, bottom). Figs. 2a–2c show TPO profiles for Pt black, ZrO_2 and, Pt/ZrO_2 catalysts exposed to a single AcOH pulse. The TPO profile for Pt black exhibits only one peak, at 438 K (Fig. 2a). The TPO profile for ZrO_2 (Fig. 2b) has one broad peak with a maximum at 670 K. In contrast, the TPO profile for Pt/ZrO_2 (Fig. 2c) shows three peaks (maxima at 433, 465, and 575 K). The presence of Pt in the catalyst considerably lowered the temperature for removal of the deposits with O_2 (compare Figs. 2b and 2c), as expected from the well-known fact that Pt is a good combustion catalyst.

We propose that the first peak in Fig. 2c originates from "C" on Pt surface based on the fact that the peak in the same temperature region is shown on Pt black (Fig. 2a). The high-temperature peak on Pt/ZrO_2 (Fig. 2c) can be ascribed to the carbon species on the support remote from Pt particles (presumably acetate/carbonate species [7,19] and oligomers). Therefore, we tentatively assign the second peak to the deposits on the perimeter of the Pt particles. Based on the bifunctional mechanism, deposits at the perimeter would be expected to affect the catalytic activity. To investigate this, we treated the used catalyst in O_2 at different temperatures.

As shown in Fig. 3, the catalytic activity for steam reforming decreased significantly after 1 h time on stream (TOS) of continuous testing (from 29.4 to 2.5 μmol g^{-1} s^{-1} for H_2 formation rate). The TPO profile for the catalyst after 1 h TOS (Fig. 2d) exhibits three peaks (maxima at 436, 476, and 580 K, respectively). Compared with the TPO profiles after the pulse treatment (Figs. 2a–2c), the high-temperature peak increased in intensity as the deposition of carbonaceous species on ZrO_2 continues, as shown by the high AcOH conversion (Fig. 3) even after deactivation for steam reforming. In contrast, the low-temperature peaks are very similar for Figs. 2c and 2d. The catalyst was then treated in O_2 at two different temperatures

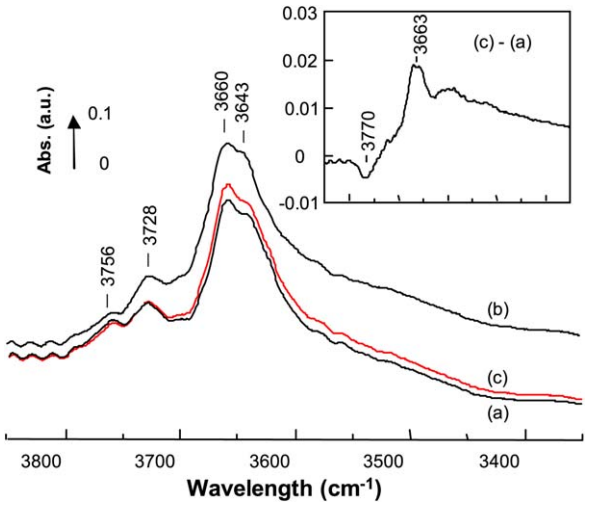

Fig. 4. IR spectra of hydroxyls on Pt/ZrO_2 at 625 K. (a) before H_2O introduction, (b) in the presence of 13 mbar H_2O, (c) after evacuation for 15 min after (b). Upper box shows difference spectrum of (c) and (a).

(435 and 475 K) for 15 min. After O_2 treatment at 435 K, the first peak disappeared from the TPO profile (Fig. 2e), but the second peak remained. However, the catalytic activity for steam reforming recovered only slightly with this treatment (Fig. 3). The fact that both the first and second peaks disappeared completely after oxidation at 475 K (Fig. 2f) and the observation that the H_2 formation rate recovered significantly from 2.5 to 18.6 $\mu mol\, g^{-1}\, s^{-1}$ (Fig. 3) support our suggestion that the periphery sites of the metal particles are kinetically relevant active sites for steam reforming.

3.4. Active species derived from H_2O on the catalyst surface for steam reforming

Based on the assumption that ZrO_2 activates water to form hydroxyl groups, IR spectra of ν(OH) region were measured when the Pt/ZrO_2 catalyst was exposed to water vapor; the spectra are shown in Fig. 4. After reduction at 775 K (before introduction of H_2O), isolated surface OH groups (at ca. 3756, 3728, 3660, and 3643 cm^{-1}) were observed [20,21]. When H_2O was introduced (1.3 kPa), intensities of all of the OH peaks increased (Fig. 4b). Even after thorough evacuation (Fig. 4c), intensities of these OH peaks were higher than those before introduction of H_2O (Fig. 4, upper figure showing the difference spectrum between c and a). Throughout the experiments, molecularly coordinated H_2O (δ_{HOH}) at ca. 1630 cm^{-1} was not observed.

It should also be noted that the state of Pt should remain the same after the introduction of H_2O, because dissociation of the O–H bond in H_2O on Pt is not thermodynamically plausible under the study conditions [22]. Therefore, it can be concluded that H_2O dissociatively adsorbs on the ZrO_2 exclusively and forms supplementary hydroxyl groups.

Table 3 gives the product distribution, from AcOH or acetone pulse, after the catalyst was either exposed or not exposed to H_2O before the pulse. In the case of AcOH, previous treatment with H_2O resulted in increased H_2, CO_2 and CH_4 yields

Table 3
Effects of water pretreatment on product distributions for AcOH or acetone pulse reaction over Pt/ZrO_2 catalysts (625 K, AcOH 3.8 μmol, acetone 4.3 μmol, H_2O 22 μmol)

Reactant	H_2O pulse prior to oxygenate pulse	Yield (μmol)				
		H_2	CO_2	CO	CH_4	Acetone
AcOH	Without	1.32	0.91	1.57	0.75	0.26
AcOH	With	1.59	1.24	1.15	0.84	0.31
Acetone	Without	0.52	0.00	0.03	0.10	–
Acetone	With	0.77	0.08	0.05	0.14	–

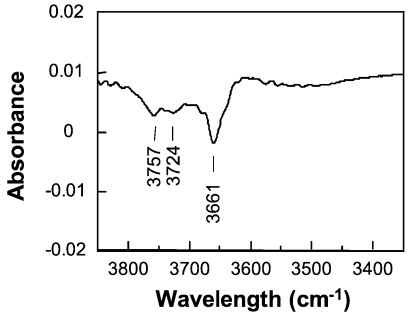

Fig. 5. IR difference spectra of hydroxyls on Pt/ZrO_2 after exposure to AcOH (0.13 kPa), referred to after H_2O treatment (1.3 kPa) and evacuation at 625 K.

and decreased CO yield, but had no effect on acetone formation. Note that the amount of oxygen in CO_x increased by 0.24 μmol. In the case of acetone pulse without H_2O pretreatment, H_2, CO, and CH_4 were formed, in agreement with results reported for Pt foil [23]. In the case of H_2O pretreatment, more H_2, CO, and CH_4 were produced, and CO_2 was also formed. Similarly, an additional 0.18 μmol of oxygen was contained in the CO_x mixture produced. Increasing oxygen content in the product must be derived from surface hydroxyl groups. Fig. 5 shows the IR difference spectrum in the ν(OH) region after introduction of AcOH. It can be seen that after the introduction of AcOH (0.13 kPa) to the catalyst pretreated with H_2O, the intensity of the peaks for surface hydroxyl groups decreased significantly. Similar results were also observed with acetone (not shown). These results confirm the participation of hydroxyl groups derived from water for steam-reforming and WGS reactions.

3.5. Kinetic relevance of possible secondary reactions during steam reforming of acetic acid

Under conditions for AcOH steam reforming, the products from AcOH decomposition (H_2, CO_x, and CH_4) may undergo secondary reactions, which can significantly affect hydrogen yield. To elucidate the kinetic relevance of the secondary reactions, separate kinetic tests for CH_4 formation (CO/H_2) and CH_4 consumption (CH_4/H_2O) were carried out over the Pt/ZrO_2 catalysts (Table 4). It was found that CO hydrogenation was kinetically much slower for methane formation, even when the reactant (CO, H_2) concentrations were considerably greater than those actually expected for the AcOH reforming (Table 1). Therefore, it is suggested that the CH_4 observed for AcOH reforming is a primary product from AcOH decomposition on Pt and is not derived from secondary CO hydrogenation.

Table 4
Production/consumption rate of hydrogen and methane over Pt/ZrO_2 for various reactions. (625 K, $H_2O/C = 5$ or $H_2/C = 3$, GHSV = 1,600,000 h^{-1})

	Initial formation/consumption rate ($\mu mol\ g^{-1}\ s^{-1}$)		
	$AcOH/H_2O$	CH_4/H_2O	CO/H_2
H_2	38	27	2
CH_4	3.6	6.6	1.1

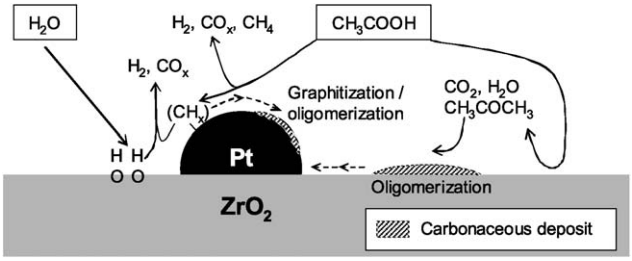

Fig. 6. The proposed pathway for the steam reforming of AcOH involving bifunctional catalysis of Pt/ZrO_2. Surface hydroxyl groups are formed from H_2O with the surface oxygen on the ZrO_2.

3.6. Mechanistic scheme for steps involved in steam reforming of AcOH

In this section, the results are compiled to arrive at a mechanistic scheme. Fig. 6 illustrates a scheme of the possible steps involved in steam reforming of AcOH over Pt/ZrO_2.

Table 2 shows that CO_2, CO, CH_4, and H_2 were formed from AcOH when Pt is present. Dumesic et al. [24] have reported both experimental results and theoretical calculations for the reactions of AcOH on Pt and suggested that the initial reactions of AcOH on Pt are the formation of acetate (step 1) or acyl (step 2) species, respectively:

$$\text{Step 1. } CH_3COOH + 2* \rightleftarrows CH_3COO* + H*. \quad (5)$$

$$\text{Step 2. } CH_3COOH + 2* \rightleftarrows CH_3CO* + OH*. \quad (6)$$

Here the symbol $*$ denotes the metal site. Then, the acetate and the acyl groups may further decompose to give CO_2 and CH_3, and CO and CH_3, respectively. The methyl can be hydrogenated with adsorbed hydrogen to form CH_4. The adsorbed hydrogen atoms can recombine to form di-hydrogen. These steps can describe formation of the decomposition products on the Pt. However, the methyl (or further dehydrogenated CH_x species, $x \leqslant 3$) can undergo graphitization and/or oligomerization. Fig. 1 shows that the deposits derived from AcOH can block the Pt surface sites to inhibit subsequent AcOH decomposition unless it is removed by H_2O (or other oxidants).

The pulse experiments (Fig. 1, Table 2) show that the activated H_2O species gasify AcOH-oriented carbon residue on the Pt to produce H_2 and CO_2, making the Pt surface available again for reaction. IR experiments (Fig. 4) show that H_2O is activated on ZrO_2 to form supplementary surface hydroxyl groups, which can participate in steam-reforming and WGS reactions (Table 3). Thus we propose that the H_2O is activated on the ZrO_2 to form surface hydroxyl groups and that the hydroxyl groups should react with CH_x species on the Pt through the Pt–ZrO_2 boundary (i.e., steam reforming). Subsequently, the WGS reaction occurs, whereas CO hydrogenation is not kinetically relevant. The importance of boundary sites is most convincingly demonstrated by the experimental result of TPO that the removal of carbon residue from the boundary sites is necessary to regenerate the catalyst for the steam reforming (Figs. 2 and 3).

Similarly, acetone may primarily decompose on Pt to form methyl and CO [23], following the steps described for AcOH (Table 3). Accordingly, we further propose here that the basic concept of this bifunctional mechanism can be applied also for steam reforming of other oxygenates; oxygenates decompose to form some gaseous products (H_2, CO_x, and CH_4) and carbonaceous residue on Pt, which subsequently reacts with hydroxyl groups on ZrO_2 derived from H_2O via the Pt–ZrO_2 boundary. The likelihood of such an event is greatest at the Pt–ZrO_2 boundary. The reason for the easier steam reforming of AcOH at lower temperatures compared with methane steam reforming (1000 K) may be due to the fact that activation of methane to CH_x ($x = 1$–3) is a difficult step; here the easier decomposition of AcOH directly generates CH_x type species.

The scheme proposed here will be operative until the boundary sites between Pt and ZrO_2 are blocked by deposits. It should be mentioned that the deposits causing deactivation may originate from CH_x formed on Pt and the acetone-derived oligomers (i.e., aldol condensation-type reactions) formed on the ZrO_2 in different pathways. Indeed, large amounts of deposits were formed from AcOH both on Pt and ZrO_2 (Table 2, Fig. 2). Because Pt/ZrO_2 is stable for hydrocarbon reforming [25], oligomer formation on ZrO_2 is more likely than coke formation on Pt to be responsible for the deactivation. It has been suggested that the oligomerization on the oxides is related to dehydration reactions [9], so that higher reactivity of the support with H_2O might prevent the oligomerization. Thus, we conclude that to improve the catalysts for steam reforming of oxygenates, in terms of both activity and durability, the support should be designed to have high affinity with H_2O and to facilitate the formation of hydroxyl groups from H_2O.

4. Conclusion

A bifunctional mechanism has been claimed for steam reforming of AcOH over Pt/ZrO_2, where Pt and ZrO_2 have roles in the activation of AcOH and H_2O. It was found that on Pt, AcOH is decomposed to release H_2, CO, CO_2, and CH_4 into the gas phase and to leave carbonaceous residue that potentially deactivates the Pt surface. The residue can be gasified with water, forming additional H_2 and CO_2 (steam reforming). IR measurement confirmed that water is activated on the ZrO_2, forming surface hydroxyl groups, which are consumed in the gasification of carbon species derived from AcOH. Based on our observations, it is proposed that the reaction must occur at the Pt–ZrO_2 boundary sites. A similar sequence of events during the steam reforming of acetone implies the generality of the concept for the bifunctional mechanism proposed for the steam reforming of oxygenates.

Acknowledgment

This work was performed under the auspices of NIOK, The Netherlands Institute for Catalysis.

References

[1] E. Chornet, S. Czernik, Nature 418 (2002) 928.
[2] A.B. Bridgwater, in: Fast Pyrolysis of Biomass: A Handbook, vol. 2, CPL Press, 2002.
[3] L. Garcia, R. French, S. Czernik, E. Chornet, Appl. Catal. A 201 (2000) 225.
[4] A.V. Bridgwater, Catal. Today 29 (1996) 285.
[5] J.R. Galdámez, L. García, R. Bilbao, Energy Fuels 19 (2005) 1133.
[6] C. Rioche, S. Kulkarni, F.C. Meunier, J.P. Breen, R. Burch, Appl. Catal. B 61 (2005) 130.
[7] K. Takanabe, K. Aika, K. Seshan, L. Lefferts, J. Catal. 227 (2004) 101.
[8] K. Takanabe, K. Aika, K. Seshan, L. Lefferts, Top. Catal., submitted for publication.
[9] K. Takanabe, K. Aika, K. Seshan, L. Lefferts, Chem. Eng. J. 120 (2006) 133.
[10] T. Milne, F. Agblevor, M. Davis, S. Deutch, D. Johnson, in: A.V. Bridgwater, D.G.B. Boocock (Eds.), Developments in Thermochemical Biomass Conversion, Blackie, Glasgow, 1997, pp. 409–424.
[11] J.R. Rostrup-Nielsen, J. Catal. 31 (1973) 173.
[12] J.R. Rostrup-Nielsen, in: J.R. Anderson, M. Boudart (Eds.), Catalysis, Science and Technology, vol. 5, Springer-Verlag, Berlin, 1984, chap. 1.
[13] D.C. Grenoble, J. Catal. 51 (1978) 203.
[14] D.C. Grenoble, J. Catal. 51 (1978) 212.
[15] D. Duprez, P. Pereira, A. Miloudi, R. Maurel, J. Catal. 75 (1982) 151.
[16] D. Duprez, Appl. Catal. A 92 (1992) 111.
[17] G.V. Dydykina, G.L. Rabinovich, G.N. Maslyanskii, M.I. Dementieva, O.M. Oranskaya, Kinet. Catal. 12 (1972) 703.
[18] D.C. Grenoble, M.M. Estadt, D.F. Ollis, J. Catal. 67 (1981) 90.
[19] W. Rachmady, M.A. Vannice, J. Catal. 207 (2002) 317.
[20] G. Cerrato, S. Bordiga, S. Barbera, C. Morterra, Appl. Surf. Sci. 115 (1997) 53.
[21] C. Morterra, L. Orio, C. Emanuel, J. Chem. Soc. Faraday Trans. 86 (1990) 3003.
[22] M.A. Henderson, Surf. Sci. Rep. 46 (2002) 1, and references therein.
[23] Z.M. Liu, M.A. Vannice, Surf. Sci. 316 (1994) 337.
[24] K.I. Gursahani, R. Alcalá, R.D. Cortright, J.A. Dumesic, Appl. Catal. A 222 (2001) 369.
[25] J.H. Bitter, K. Seshan, J.A. Lercher, J. Catal. 176 (1998) 93.